nature cell biology

SUPPLEMENTARY INFORMATION

https://doi.org/10.1038/s41556-018-0090-7

In the format provided by the authors and unedited.

Spatial orchestration of mitochondrial translation and OXPHOS complex assembly

Stefan Stoldt[1], Dirk Wenzel[2], Kirsten Kehrein[3], Dietmar Riedel[2], Martin Ott[3] and Stefan Jakobs[1,4]*

[1]Department of NanoBiophotonics, Max Planck Institute for Biophysical Chemistry, Göttingen, Germany. [2]Laboratory of Electron Microscopy, Max Planck Institute for Biophysical Chemistry, Göttingen, Germany. [3]Department of Biochemistry and Biophysics, Stockholm University, Stockholm, Sweden. [4]Department of Neurology, University Medical Center Göttingen, Göttingen, Germany. *e-mail: sjakobs@gwdg.de

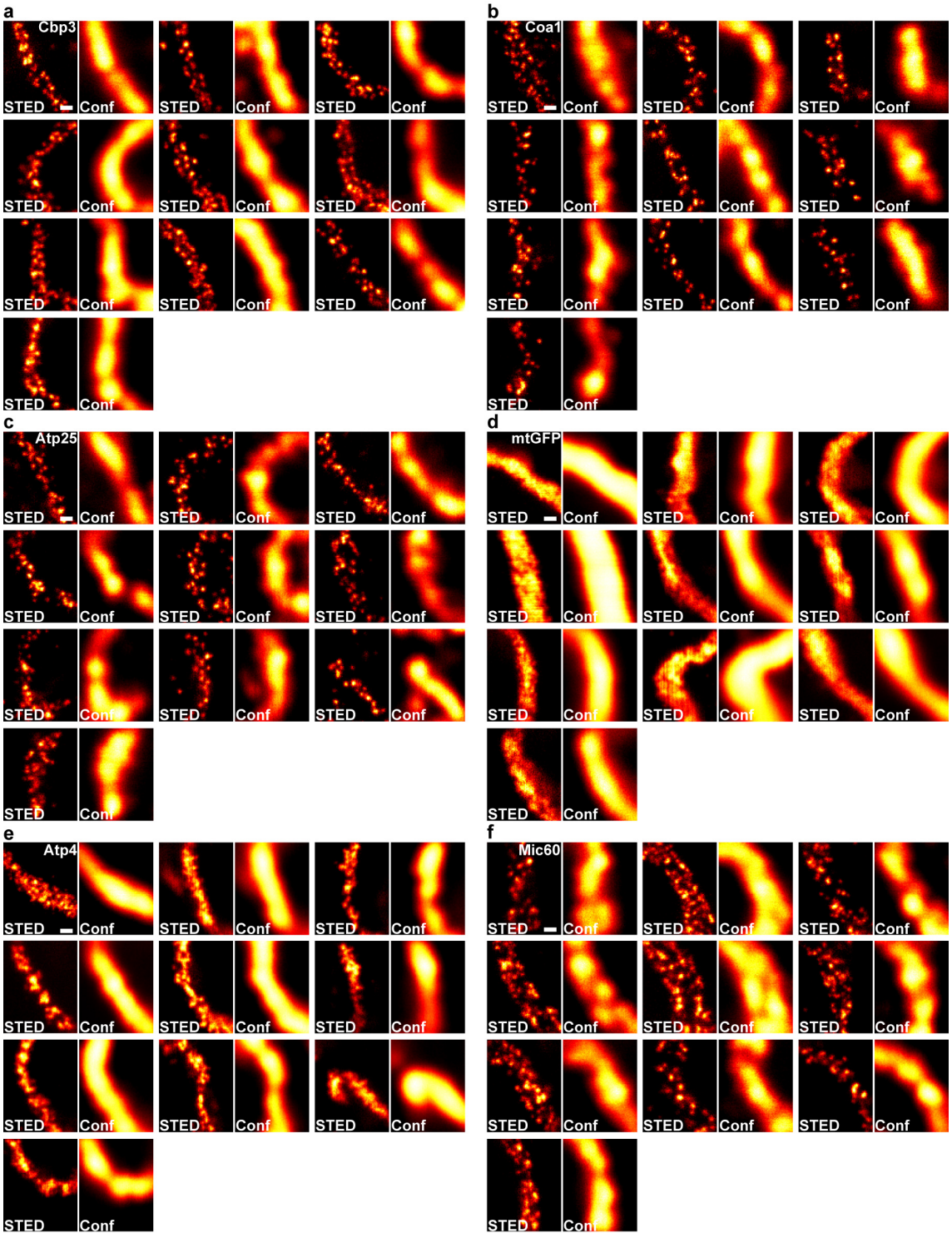

Supplementary Figure 1

Distribution of selected proteins along the mitochondrial tubules.

Images of representative mitochondrial segments of ten different yeast cells expressing Cbp3-GFP (a), Coa1-GFP (b), Atp25-GFP (c), mitochondria targeted GFP (mtGFP) (d), Atp4-GFP (e), and Mic60-GFP (f) fusion proteins from the respective endogenous genomic

locus (or from a plasmid in case of mtGFP). Cells were immunolabelled with an antiserum against GFP and imaged with STED nanoscopy and diffraction limited confocal microscopy, as indicated. All nanoscopy experiments were done in triplicate, persistently giving similar results. Scale bars: 200 nm.

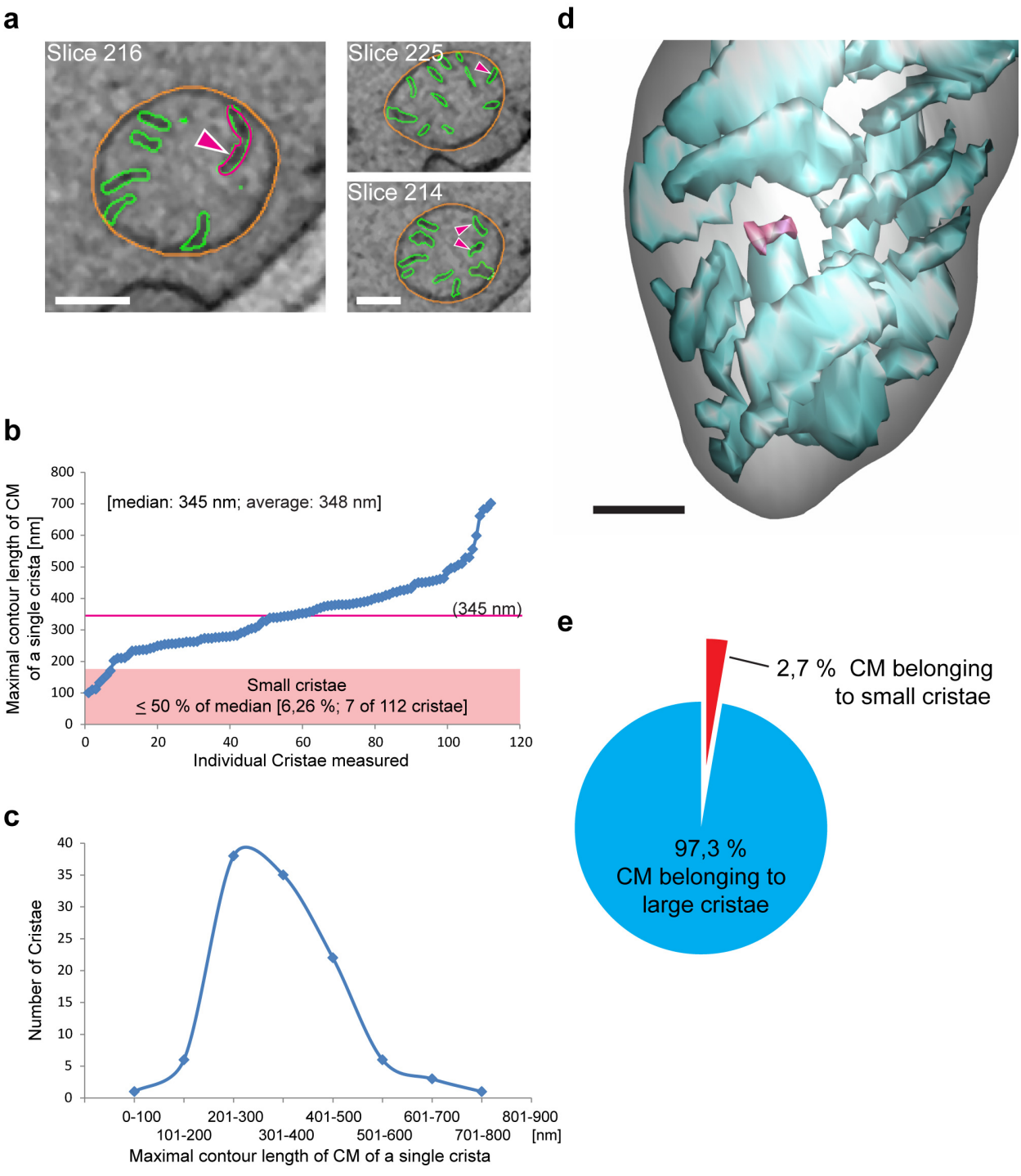

Supplementary Figure 2

The majority of all CM fragments seen on 2D slices are part of larger cristae.

For the analysis, a FIB-SEM data stack recorded on wild type S. cerevisiae cells grown in galactose medium was scrutinized. We recorded one FIB-SEM stack containing several dozen yeast cells and we reconstructed mitochondrial membranes out of three cells, all displaying similar ultrastructures. (a) We define the size of a given crista as the largest contour length of this crista in a 2D section; by

this, we will underestimate the size of very large cristae, but will reliably detect all small cristae. To determine the largest contour length of an individual crista, we analyzed 2D sections in a reconstructed 3D FIB-SEM data stack. Only the largest contour length of a crista was used for further analysis. The analysis was performed on mitochondria of two randomly chosen cells, giving similar results. In the example given in (a), the arrowheads point to the same crista in different slices of the FIB-SEM data stack. The contour length of the crista shown in slice 216 (marked in magenta) is used to characterize this crista. (The mitochondrial outer membrane is depicted in orange, the CMs in green). (b) Distribution of measured largest contour lengths of cristae. 112 cristae in two different cells were analyzed. Note that only ~6 % (7 in 112 cristae) were smaller than 50 % of the median. We define these cristae as small cristae. (c) The contour lengths of the cristae were arranged into classes and the frequency of these classes is shown. (d) A part of the mitochondrial network (21 slices) that incorporates the largest of the small cristae (see a-c) was reconstructed in 3D. The small crista is highlighted in magenta, all other cristae in cyan, the outer mitochondrial membrane in light gray. (e) The CM lengths in the 21 2D slices that lead to the 3D reconstruction shown in (d) were measured. The pie-chart displays the amount of CMs belonging to large cristae (blue) and small cristae (red). Scale bars: 200 nm (a), 100 nm (d).

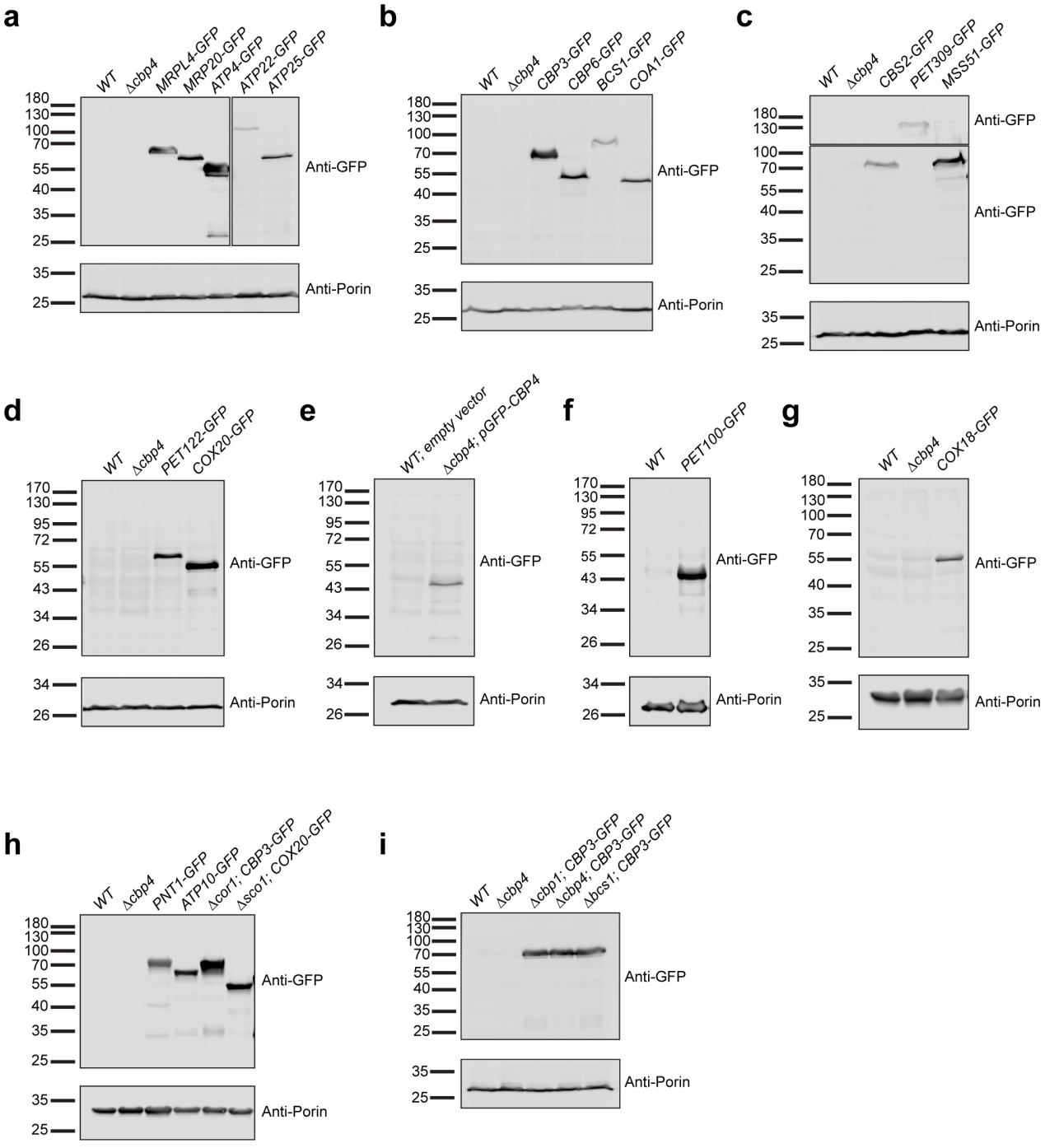

Supplementary Figure 3

The expressed fusion proteins did not exhibit notable degradation.

Shown are Western Blots of whole cell extracts decorated with an antiserum against GFP, as indicated. As a loading control of each western blot, a porin specific serum was used. Outlines indicate different exposure times that were used to ensure optimal signal to noise ratios for proteins with different expression levels on the same blot. All experiments were repeated at least two times with similar results. The full blots are shown in Supplementary Figure 6.

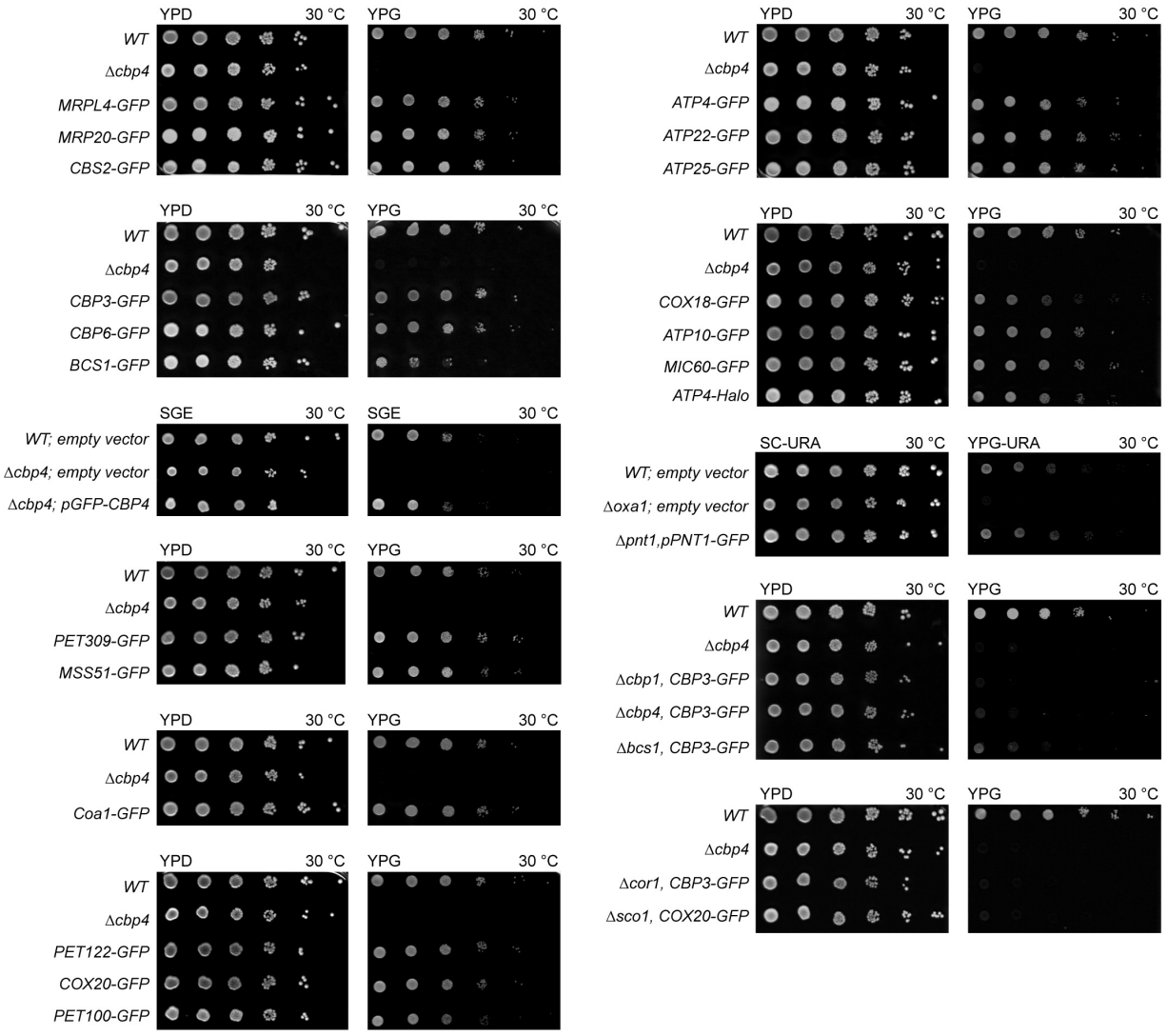

Supplementary Figure 4

Genomic tagging of the proteins of interest with GFP did not influence respiration.

Ten-fold dilutions of logarithmically growing cells with the indicated genotypes were spotted onto agar plates containing glucose (YPD; fermentable), glycerol (YPG; non-fermentable) or glycerol/ethanol (SGE; non-fermentable) as the carbon sources. All experiments were repeated at least two times with similar results. The plates were incubated for 4 d at 30 °C before photography.

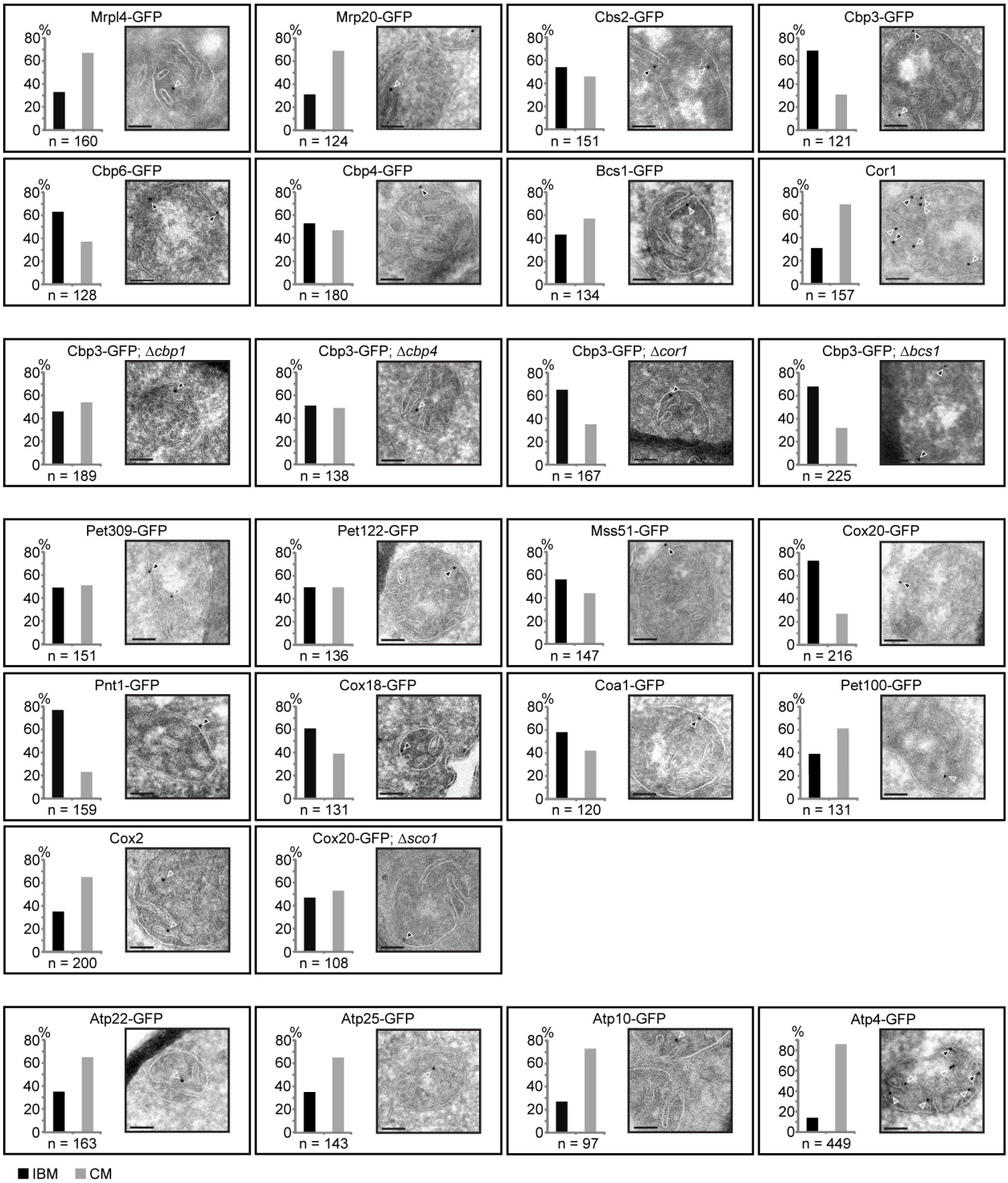

Supplementary Figure 5

Quantitative immuno-gold EM of mitochondrial proteins on cryo-sectioned cells.

Shown are representative EM images (right) and the quantifications taken from a larger number of images (left). The distributions of Cor1 and Cox2 were determined with antiserum against these proteins; all other sections

were decorated with antiserum against GFP. Cells were grown at 30 °C in galactose containing medium. The arrowheads point to gold particles at the IBM (black) or at the CM (grey). For each analyzed protein localization, at least three individual slices were decorated and analyzed; n indicates the number of analyzed gold particles. Scale bars: 100 nm.

Unprocessed gel blot images of Supplementary Figure 3

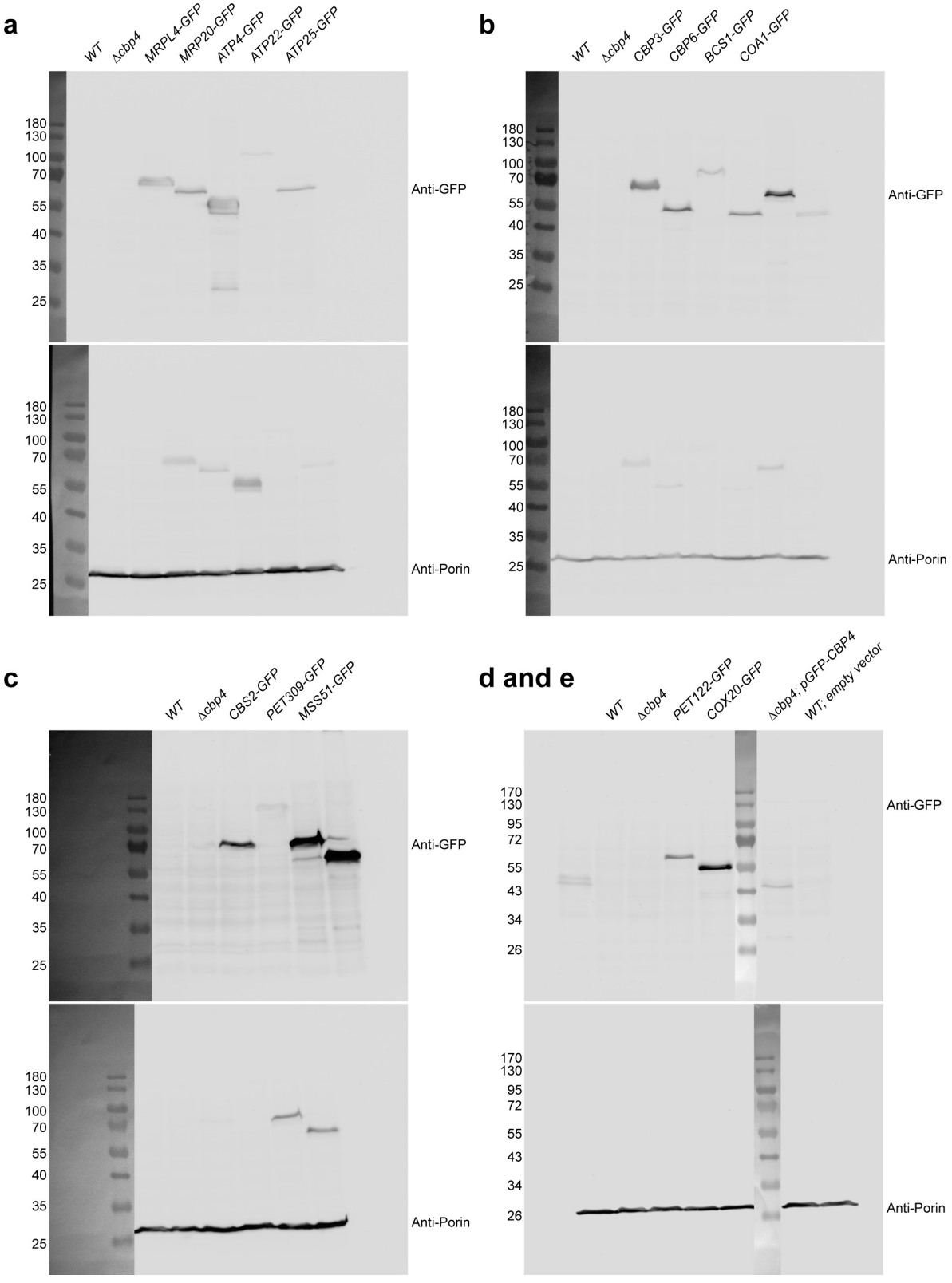

Supplementary Figure 6. Unprocessed images of all gels and blots.

Unprocessed blot images of Supplementary Figure 3.

(a-i) corresponds to the labelling in Supplementary Figure 3. Reflected light images of the blot membranes containing the size marker are combined with the camera images of the recorded enhanced chemiluminescence (ECL) signals. Membranes were not cut.

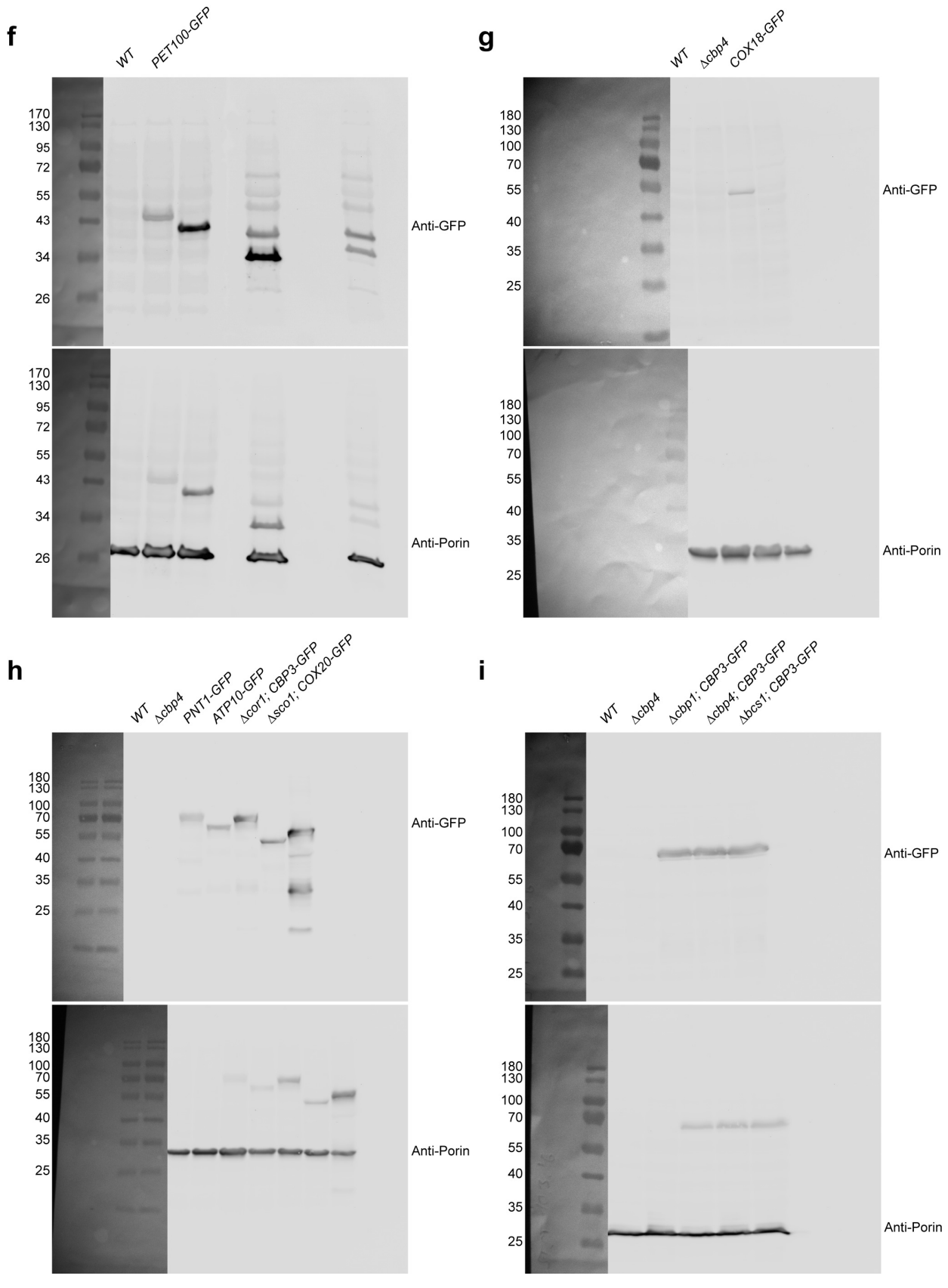
f
WT
PET100-GFP
170
130
95
72
55
43
34
26
Anti-GFP
Anti-Porin
g
WT
Δcbp4
COX18-GFP
180
130
100
70
55
40
35
25
Anti-GFP
Anti-Porin
h
WT
Δcbp4
PNT1-GFP
ATP10-GFP
Δcor1; CBP3-GFP
Δsco1; COX20-GFP
Anti-GFP
Anti-Porin
i
WT
Δcbp4
Δcbp1; CBP3-GFP
Δcbp4; CBP3-GFP
Δbcs1; CBP3-GFP
Anti-GFP
Anti-Porin

Supplementary Figure 6. Unprocessed images of all gels and blots (Continued)

Unprocessed blot images of Supplementary Figure 3.

(a-i) corresponds to the labelling in Supplementary Figure 3. Reflected light images of the blot membranes containing the size marker are combined with the camera images of the recorded enhanced chemiluminescence (ECL) signals. Membranes were not cut.

Supplementary Movie 1. Mitochondrial inner architecture. Animated overview of the source FIB-SEM data stack and the mitochondrial membrane reconstructions shown in Fig. 2. The yeast cells were grown to the logarithmic phase in galactose containing growth medium at 30 °C.

Supplementary Table 1. Proteins investigated in this study and their role in mitochondrial translation and OXPHOS assembly.

Supplementary Table 2. Primary antibodies used in this study. Corresponding references, applications, dilutions and validations. WB: Western blot, IF: Immunofluorescence, EM: Electron microscopy.

Supplementary Table 3. Primers used for epitope tagging and gene knock-outs.

Supplementary References to Supplementary Table 1

1. Gruschke, S. *et al.* Proteins at the Polypeptide Tunnel Exit of the Yeast Mitochondrial Ribosome. *Journal of Biological Chemistry* **285**, 19022-19028 (2010).
2. Amunts, A. *et al.* Structure of the yeast mitochondrial large ribosomal subunit. *Science* **343**, 1485-1489 (2014).
3. Krause-Buchholz, U., Barth, K., Dombrowski, C. & Rodel, G. Saccharomyces cerevisiae translational activator Cbs2p is associated with mitochondrial ribosomes. *Curr Genet* **46**, 20-28 (2004).
4. Gruschke, S. *et al.* Cbp3-Cbp6 interacts with the yeast mitochondrial ribosomal tunnel exit and promotes cytochrome b synthesis and assembly. *J Cell Biol* **193**, 1101-1114 (2011).
5. Gruschke, S. *et al.* The Cbp3-Cbp6 complex coordinates cytochrome b synthesis with bc(1) complex assembly in yeast mitochondria. *J Cell Biol* **199**, 137-150 (2012).
6. Kronekova, Z. & Rodel, G. Organization of assembly factors Cbp3p and Cbp4p and their effect on bc(1) complex assembly in Saccharomyces cerevisiae. *Curr Genet* **47**, 203-212 (2005).

7. Sawamura, R., Ogura, T. & Esaki, M. A conserved alpha helix of Bcs1, a mitochondrial AAA chaperone, is required for the Respiratory Complex III maturation. *Biochem Biophys Res Commun* **443**, 997-1002 (2014).
8. Hunte, C., Koepke, J., Lange, C., Rossmanith, T. & Michel, H. Structure at 2.3 A resolution of the cytochrome bc(1) complex from the yeast Saccharomyces cerevisiae co-crystallized with an antibody Fv fragment. *Structure* **8**, 669-684 (2000).
9. Zamudio-Ochoa, A., Camacho-Villasana, Y., Garcia-Guerrero, A.E. & Perez-Martinez, X. The Pet309 pentatricopeptide repeat motifs mediate efficient binding to the mitochondrial COX1 transcript in yeast. *RNA Biol* **11**, 953-967 (2014).
10. Naithani, S., Saracco, S.A., Butler, C.A. & Fox, T.D. Interactions among COX1, COX2, and COX3 mRNA-specific translational activator proteins on the inner surface of the mitochondrial inner membrane of Saccharomyces cerevisiae. *Molecular biology of the cell* **14**, 324-333 (2003).
11. Perez-Martinez, X., Butler, C.A., Shingu-Vazquez, M. & Fox, T.D. Dual functions of Mss51 couple synthesis of Cox1 to assembly of cytochrome c oxidase in Saccharomyces cerevisiae mitochondria. *Molecular biology of the cell* **20**, 4371-4380 (2009).
12. Elliott, L.E., Saracco, S.A. & Fox, T.D. Multiple roles of the Cox20 chaperone in assembly of Saccharomyces cerevisiae cytochrome c oxidase. *Genetics* **190**, 559-567 (2012).
13. Saracco, S.A. & Fox, T.D. Cox18p is required for export of the mitochondrially encoded Saccharomyces cerevisiae cox2p C-tail and interacts with Pnt1p and Mss2p in the inner membrane. *Molecular biology of the cell* **13**, 1122-1131 (2002).
14. Pierrel, F. *et al.* Coa1 links the Mss51 post-translational function to Cox1 cofactor insertion in cytochrome c oxidase assembly. *EMBO J* **26**, 4335-4346 (2007).
15. Forsha, D., Church, C., Wazny, P. & Poyton, R.O. Structure and function of Pet100p, a molecular chaperone required for the assembly of cytochrome c oxidase in Saccharomyces cerevisiae. *Biochem Soc Trans* **29**, 436-441 (2001).
16. Taanman, J.W. & Capaldi, R.A. Purification of yeast cytochrome c oxidase with a subunit composition resembling the mammalian enzyme. *J Biol Chem* **267**, 22481-22485 (1992).
17. Zeng, X., Hourset, A. & Tzagoloff, A. The Saccharomyces cerevisiae ATP22 gene codes for the mitochondrial ATPase subunit 6-specific translation factor. *Genetics* **175**, 55-63 (2007).
18. Rak, M. *et al.* Regulation of mitochondrial translation of the ATP8/ATP6 mRNA by Smt1p. *Molecular biology of the cell* **27**, 919-929 (2016).
19. Zeng, X., Barros, M.H., Shulman, T. & Tzagoloff, A. ATP25, a new nuclear gene of Saccharomyces cerevisiae required for expression and assembly of the Atp9p subunit of mitochondrial ATPase. *Molecular biology of the cell* **19**, 1366-1377 (2008).
20. Woellhaf, M. W., Sommer, F., Schroda, M. & Herrmann, J. M. Proteomic profiling of the mitochondrial ribosome identifies Atp25 as a composite mitochondrial precursor protein. *Mol Biol Cell* **27**, 3031-3039 (2016).
21. Tzagoloff, A., Barrientos, A., Neupert, W. & Herrmann, J.M. Atp10p assists assembly of Atp6p into the F0 unit of the yeast mitochondrial ATPase. *J Biol Chem* **279**, 19775-19780 (2004).
22. Rak, M., Gokova, S. & Tzagoloff, A. Modular assembly of yeast mitochondrial ATP synthase. *EMBO J* **30**, 920-930 (2011).
23. Naumenko, N., Morgenstern, M., Rucktaschel, R., Warscheid, B. & Rehling, P. INA complex liaises the F1Fo-ATP synthase membrane motor modules. *Nat Commun* **8**, 1237 (2017).